Protons accumulation during anodic phase turned to advantage for oxygen reduction during cathodic phase in reversible bioelectrodes

Elise Blanchet, Sophie Pécastaings, Benjamin Erable, Christine Roques, Alain Bergel

Protons accumulation during anodic phase turned to advantage for oxygen reduction during cathodic phase in reversible bioelectrodes

Elise Blanchet [a,*], Sophie Pécastaings [b], Benjamin Erable [a], Christine Roques [b], Alain Bergel [a]

[a] Laboratoire de Génie Chimique (LGC), CNRS, Université de Toulouse (INPT), 4 allée Emile Monso, BP 84234, 31432 Toulouse, France
[b] Laboratoire de Génie Chimique, BioSym Department, Université de Toulouse, 35 chemin des Maraîchers, 31062 Toulouse, France

HIGHLIGHTS

- Reversible bioelectrodes were designed under polarization at −0.20 V vs. SCE.
- The bioelectrodes catalyzed both acetate oxidation and oxygen reduction.
- Proton accumulation during anodic phase enhanced oxygen reduction by the biocathode.
- Microbial community was dominated by Chloroflexi (49%).

ABSTRACT

Reversible bioelectrodes were designed by alternating acetate and oxygen supply. It was demonstrated that the protons produced and accumulated inside the biofilm during the anodic phase greatly favored the oxygen reduction reaction when the electrode was switched to become the biocathode. Protons accumulation, which hindered the bioanode operation, thus became an advantage for the biocathode. The bioanodes, formed from garden compost leachate under constant polarization at −0.2 V vs. SCE, were able to support long exposure to forced aeration, with only a slight alteration of their anodic efficiency. They produced a current density of 16 ± 1.7 A/m^2 for acetate oxidation and up to −0.4 A/m^2 for oxygen reduction. Analysis of the microbial communities by 16S rRNA pyrosequencing revealed strong selection of Chloroflexi (49 ± 1%), which was not observed for conventional bioanodes not exposed to oxygen. Chloroflexi were found as the dominant phylum of electroactive biofilms for the first time.

Keywords:
Microbial fuel cell
Biocathode
Reversible electrode
Oxygen reduction
Chloroflexi

1. Introduction

Microbial fuel cells (MFCs) are seen as a promising technology for producing electricity directly from the oxidation of various organic compounds that can be obtained at low cost and in sustainable way. The most widely studied MFC architectures are composed of a microbial anode associated with an abiotic oxygen-reduction cathode. Unfortunately, abiotic air–cathodes still give a rather low rate of oxygen reduction at the neutral pH values that are required for the microbial anodes. This problem remains an essential stumbling block in the development of large MFCs. Up to now, the power density provided by MFCs equipped with abiotic oxygen-reducing air cathodes has levelled off around 7 W/m^2 (Fan et al., 2008; Borole et al., 2011; Pocaznoi et al., 2012b) for small-sized cells and decreases drastically as soon as the system size increases (Santoro et al., 2013).

An appealing alternative solution would be to implement oxygen-reduction microbial cathodes (Erable et al., 2012), which have already proved their remarkable efficiency (Carbajosa et al., 2010). However, a major drawback of associating a microbial anode with a microbial cathode is that a pH gradient is established between the anode and cathode compartments. The pH gradient is the result of the production of protons at the anode as, for instance, in the widely used oxidation of acetate:

$$CH_3COO^- + 4H_2O \rightarrow 2HCO_3^- + 9H^+ + 8e^- \quad (1)$$

Coupled with the production of hydroxide ions by oxygen reduction at the cathode:

$$2O_2 + 4H_2O + 8e^- \rightarrow 8OH^- \quad (2)$$

* Corresponding author. Tel.: +33 5 34323626.
E-mail address: blanchet.elise@gmail.com (E. Blanchet).

http://dx.doi.org/10.1016/j.biortech.2014.09.076

Ideally, electro-neutrality should be maintained by proton migration to the cathode compartment and hydroxide ion migration to the anode compartment, but the diffusion of these ions is too slow with respect to the other ions contained in the electrolytes (sodium, potassium, chloride, acetate, phosphate and carbonate ionic species, etc.) and proton migration plays only a minor role in charge-balancing. The pH gradient has been identified as a major source of losses in the performance of microbial electrochemical systems (Harnisch and Schröder, 2009). Membrane-less cells may provide part of the solution by decreasing the hindrance to ionic transport but, in return, they reduce electron recovery because of the direct aerobic conversion of the organic fuel due to oxygen diffusion from the cathode side (Rozendal et al., 2008). The use of a chemical buffer can compensate for the deficiency of proton transport (Torres et al., 2008), but it would be costly on a large scale. Freguia et al. (2008) addressed the problem by proposing a loop configuration: the effluent from the anode compartment was directed to the cathode compartment. This operating mode largely solved the problem of the pH gradient and it also improved the cathode performance compared with an abiotic oxygen cathode. However, such a system requires careful operation to avoid excessive chemical oxygen demand (COD) entering the cathode, which would cause the growth of aerobic heterotrophs and eventually restrict oxygen supply to the cathode biofilm.

Cheng et al. (2010) proposed the use of a reversible bioelectrode to avoid the problem of pH gradient and to improve the oxygen reduction catalysis. They showed that it was possible for a biofilm formed from activated sludge to catalyze both the anodic substrate oxidation and the cathodic oxygen reduction. The proposed MFC was operated in sequential phases by supplying acetate and oxygen to the electrode alternately. This system offers the advantage of avoiding growth of aerobic heterotrophic bacteria by separating acetate and oxygen supplies. Moreover, the protons accumulated during the anodic reaction do not need to be transported out of the biofilm: they stimulate the subsequent cathodic reaction. The concept of a reversible electrode has also been proposed by Strik et al. (2010), who used a reversible electrode inoculated with sludge to design a solar energy powered MFC. More recently, Li et al. (2014) have described a dual bioelectrode MFC with periodic reversal of polarity which results in a 36% increase in power density compared to that produced by the MFC without polarity reversal.

Reversible microbial anodes may be a very good solution to overcome the problem of pH gradient. The proton accumulation that occurs during the anodic phase (Reaction 1) prepares favorable conditions for oxygen reduction during the cathodic phase (Reaction 2). Despite their obvious advantages, studies of such reversible microbial electrodes remain rare and, in particular, little is known about the microbial composition of such intriguing biofilms, which are able to ensure an anaerobic anode respiring process and catalysis of oxygen reduction alternately. No comprehensive description of the microbial population of reversible electroactive biofilms has been published so far.

The purpose of the present work was to assess the capability of garden compost to form such reversible microbial electrodes. This inoculum source has already led to very efficient microbial anodes (Ketep et al., 2014) and has also been shown to contain bacterial strains (members of *Enterobacter* and *Pseudomonas* genera) with the ability to catalyze the electrochemical reduction of oxygen (Parot et al., 2009). Consequently, this inoculum was a priori an excellent candidate to form reversible microbial electrodes and the results presented here confirm this hypothesis. The reversible microbial electrodes formed here were then used for the in-depth analysis of the microbial communities. From a practical point of view, reversible bioelectrodes made from a soil inoculum may also open up interesting possibilities for designing plant-MFCs (Strik et al., 2008).

All experiments were performed in a 3-electrode set-up so as to accurately characterize the electrode behavior. Actually, in whole MFC set-ups, the potential of the working electrode vary considerably, which adds a source of deviation between one experimental device and another. Since the reversible bioelectrode concept was still in its infancy, it was chosen to work in well-controlled analytical conditions here, in order to focus on the electrode behavior, rather than repeating a proof of concept with a whole MFC set-up, as already reported (Freguia et al., 2008; Li et al., 2014). Following this line of thought, electrodes with small surface areas were implemented in large volumes of electrolyte to ensure experimental conditions that favored electrode performance (Rimboud et al., 2014). The bioelectrodes were formed under constant polarization at −0.2 V vs. SCE. Their electrochemical properties were characterized by cyclic voltammetry and their microbial communities were analyzed by 16S rRNA pyrosequencing.

2. Methods

2.1. Medium and inoculum: garden compost leachate

Commercial garden compost was used as a source of electroactive microorganisms. 1.5 L of an aqueous solution containing 60 mM KCl was mixed with 1 L of garden compost and stirred for 24 h at room temperature. The mixture was then percolated through a felt cloth to eliminate non-soluble macroparticles. The final leachate was used as the electrolyte in the electrochemical reactors after supplementation with 20 mM acetate. The initial pH was 7.8 and the experiments were performed at 40 °C as already optimized by Cercado-Quezada et al. (2010).

2.2. Electrochemical set-up

Experiments were performed in single compartment electrochemical reactors equipped with a 3-electrode system composed of an 8 cm^2 carbon cloth working electrode (PaxiTech, Grenoble) connected with a platinum wire, a saturated calomel reference electrode (SCE, Radiometer Analytical, +0.241 V vs. SHE) and an 8 cm^2 Pt grid as auxiliary electrode. The working electrode was located far (around 10 cm) from the auxiliary electrode but as close as possible (around 0.5 cm) to the reference electrode. Each reactor contained 600 mL of compost leachate. The working electrodes were polarized at −0.20 V vs. SCE using a multi-channel VSP potentiostat (Bio-Logic SA, software EC-Lab) and the current was recorded every 10 min. Chronoamperometry was sometimes interrupted to perform cyclic voltammetry at low scan rate (1 mV/s) in the range −0.6 to +0.3 V vs. SCE.

Coulombic efficiencies (CE) were calculated as the ratio of the experimental electric charge passing through the system, obtained by integrating the current over time, and the theoretical charge calculated by assuming that 1 mol of acetate produces 8 mol of electrons according to the oxidation reaction (1).

2.3. Development of the reversible bioelectrode

Two experiments were systematically carried out in parallel (duplicates) to validate the reproducibility of the results. In the running of the electrochemical reactors, periods of acetate supply alternate with periods of oxygen supply. Acetate was added as a pulse of 3 mL of 4 M sodium acetate solution. Oxygen was supplied by forced aeration of the solution.

Step 1 (anode, day 1 to day 10) intended to form the microbial anode with two successive pulses of 20 mM acetate; the second pulse was added when the current had returned to zero because of acetate depletion. The acetate concentration was monitored by an enzymatic kit (K-ACETAK, Megazyme).
Step 2 (cathode, day 10 to day 24) corresponded to the intermittent introduction of air. To confirm the oxygen dependence of the cathodic current recorded on the microbial electrode, air was not introduced continuously during this phase.
Step 3 (anode, day 24 to day 34) started with the addition of the third 20 mM pulse of acetate.
Step 4 (cathode, day 34 to day 44) began after the acetate from step 3 was totally depleted. Air was then introduced continuously from day 34 to day 38. Aeration was turned off from day 38 to day 42 and the reactor was left open to the air. Finally, a new period of forced aeration was tested from day 42 to the end (day 44).

2.4. Bacterial community analyses

The sample of garden compost leachate used to fill the reactors was referred as T0-inoc. At the end of the experiments (day 44), samples of 2 mL were collected from both reactors and referred as Bulk 1 and Bulk 2. At the end of the experiments, the biofilms were also collected from the electrodes by sonication in 2 mL of distilled water (3 min at a power level of 80 W), and referred as Biofilm 1 and 2. Cells were concentrated by centrifugation and re-suspended in 500 µL of water. The DNA was extracted from 250 µL of each sample using the MOBIO PowerSoil® DNA Isolation kit according to the manufacturer's instructions.

DNA extractions were also performed with the PowerBiofilm® DNA Isolation Kit (MOBIO) and pyrosequencing results confirmed the consistency of the DNA extractions achieved with the 2 kits. Both kits are able to extract good quality DNA in a reproducible manner.

DNA concentrations and purity were checked by reading the absorbance at 260 and 280 nm. Samples were sent to Research and Testing Laboratory (RTLab – Texas, USA) where 454 pyrosequencing (Roche) was performed with primers 28F (5′-GAG TTT GAT YMT GGC TC-3′) and 519R (5′-GWA TTA CCG CGG CKG CTG-3′).

Microbial diversity screening and data processing were carried out at Research and Testing Laboratory (Lubbock TX) using methods described previously (Dowd et al., 2008). Raw data were screened and trimmed based on quality scores. Sequences shorter than 250 bp were removed. Reads were classified into clusters using USEARCH (Edgar, 2010). After sequencing, individual collections of sequences were depleted of chimeras using UCHIME (Edgar et al., 2011).

Tentative identification of bacterial species was performed using BLASTN in comparison with a curated high-quality 16S rRNA gene database from the National Center for Biotechnology Information (NCBI). The compiled data were used to determine the relative percentages of bacteria for each individual sample.

Sequences >97% identity to known or well-characterized 16S rRNA sequences (<3% divergence) were resolved at the species level, between 95% and 97% at the genus level, between 90% and 95% at the family level, and between 80% and 90% at the order level.

To assess the diversity of the microbial population in the bulks and biofilms of the study, Simpson's reciprocal indexes were calculated from the number of operational taxonomic units (OTUs) assigned at the species level, according to the equation:

$$\text{Simpson} = 1 - \frac{\sum_{i=1}^{S} ni * (ni-1)}{N * (N-1)} \quad (3)$$

where *ni* is the number of sequences belonging to the ith OTU (>97% identity) and *N* is the total number of sequences that remain for the sample after quality control. *S* is the number of OTUs.

3. Results and discussion

3.1. Bioanode formation and consequences of aerobic phase on the bioanode performance

Electrochemically active biofilms were initially formed in the presence of acetate on the surface of carbon cloth electrodes immersed in garden compost leachate and polarized at −0.20 V vs. SCE. After 3 days of polarization, current densities started to increase and reached a maximum of 7.6 ± 0.7 A/m^2 and then felt down again to zero because of acetate depletion (Fig. 1). On the 6th day, a second acetate injection (20 mM) caused the current to increase to 19.3 ± 1.4 A/m^2 in less than 2 days. To obtain a mature bioanode, i.e., an anode giving fairly stable maximum current densities, it is considered that 4 successive acetate additions are necessary (Pocaznoi et al., 2012a). Only two acetate pulses were applied here as the choice had been made not to allow the biofilm to reach full maturity, in order to have the highest chance of adapting a young biofilm to aerobic conditions. Forced aeration was started in the reactor on the 10th day when the oxidative current was close to zero. The first cathodic phase lasted for 14 days.

From day 24, aeration was stopped and acetate 20 mM was added to the reactor. Oxidation current started to increase after 3 ± 1 days of latency. The lag-phase for this third pulse was longer than the previous one, because some time was necessary for the microorganisms to re-adapt from aerobic conditions to the anode-respiring function. Then, current density reached a maximum of 16 ± 1.7 A/m^2. After air exposure, the current density was lower than could have been expected considering the current density obtained with the second pulse (average of 19.3 A/m^2). It has been previously reported that the current density increased with a third pulse of acetate, due to the biofilm growth (Cercado et al., 2013).

The aerobic phase affected the bioanode performance slightly by increasing the lag-time before current generation and by decreasing the maximum current density a little. It may be speculated that the microbial community was impacted by the death of the strictly anaerobic bacteria. Nevertheless, the two-week aerobic phase did not compromise the capacity of the biofilm to achieve efficient acetate oxidation through anode respiration. To our

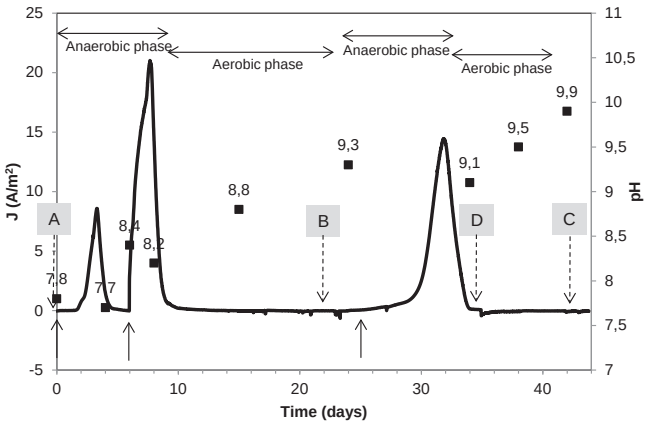

Fig. 1. Chronoamperometry and pH values in reactor 1. Current density recorded on carbon cloth electrode polarized at −0.20 V vs. SCE in a compost leachate supplemented with 20 mM of acetate. Letters A–D with dotted arrows correspond to the voltammograms of Figs. 3 and 5. Plain arrows indicate 20 mM acetate pulse.

knowledge, this is the first time that such a reversible bioelectrode has been designed using an inoculum coming from soil, and it provided good robust performance. Current density of 16 A/m^2 was reached for acetate oxidation, even after a considerable aerobic period.

On Fig. 1 is also displayed measured pH in the solution. General trend is alkalinization throughout the experiment (from 7.8 to 9.9). According to (Pocaznoi et al., 2012b), this alkalinization is not linked to the electrochemical reactions but was due to the spontaneous evolution of the non-buffered compost leachate. Momentary acidification of the solution can be observed when acetate is consumed.

Coulombic efficiency (CE) increased from 7.5% ± 1.5% to 32.5 ± 1.5% for the first and the second pulses, respectively. It reached 35 ± 3% for the third acetate pulse. These values resulted from the balance between the anode-respiring processes and the consumption of acetate by metabolic pathways that did not use the anode. Values lower than 50% indicated that much of the acetate was oxidized by using alternative electron acceptors instead of the electrode. As already discussed elsewhere (Cercado et al., 2013), a rich medium such as garden compost contains alternative dissolved electron acceptors (nitrate, sulfate, etc.), which are detrimental to CE. The dissolved oxygen was another alternative electron acceptor, as no particular care was taken to restore strict anaerobic conditions in the reactors after the forced aerobic period. Finally, the working electrode surface area (8 cm^2) was small relative to the total volume of solution in the system (600 mL). Such a design was chosen to favor the production of high currents, and it succeeded in this objective, but it is known to be detrimental to Coulombic efficiencies (Ketep et al., 2013; Rimboud et al., 2014).

3.2. Catalysis of oxygen reduction

After the third pulse of acetate at day 24, the electrodes were again subjected to forced aeration on day 35. Fig. 2 presents the evolution of the current density in reactor 1 during this second aerobic phase. It corresponds to a zoom-in of the Fig. 1 between day 34 and 44. When oxygen was provided, the electrodes immediately acted as biocathodes, with reduction currents up to −400 mA/m^2 (Fig. 2 – zone 1), which are among the highest reported so far for oxygen reduction in a medium fed with air at neutral pH (Erable et al., 2012). The reduction current then decreased over time (24 h) to reach a stable value around 71 mA/m^2. This stable value

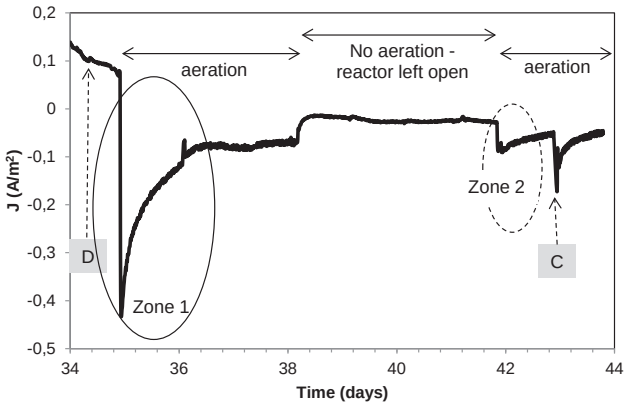

Fig. 2. (Zoom in on Fig. 1): Chronoamperometry of the second cathodic phase (from day 34 to day 44) in reactor 1. A continuous forced aeration was implemented from day 34 to day 38 (Zone 1), aeration was turned off between days 38 and 42 and the reactor was left open to the air and aeration was resumed on day 42 to the end (Zone 2). There was no acetate feeding (and consequently no anodic phase) prior to Zone 2. Letters C and D with dotted arrows correspond to the cyclic voltammetries represented in Fig. 5.

at an applied potential of −0.20 V vs. SCE was slightly smaller than values reported previously for oxygen-reducing biocathodes formed in seawater: around 100 mA/m^2 at 0.0 V vs. Ag/AgCl (Dumas et al., 2008), and 250 mA/m^2 at −0.10 V vs. SCE (Bergel et al., 2005). The biocathodes formed here produced fair, but not exceptional, stable current densities (71 mA/m^2) but they exhibited great transient performance (400 mA/m^2) just after having been switched from anode to cathode operation. Alternating anode and cathode phases drastically improved the efficiency of the biocathode.

The high transient performance and its subsequent disappearance could be explained by changes in the local pH in the biofilm. During the anodic phase, the oxidation of acetate produced a considerable amount of protons (Reaction 1), which accumulated inside the biofilm (Torres et al., 2008). The biofilm thus had a local pH significantly lower than that of the solution bulk when the electrode started to be exposed to aeration. According to the diffusion model of Torres et al. (2008), considering the current density of 16 A/m^2 and the measured pH in the solution of 9.1 just before the exposition to oxygen (day 34), and considering a biofilm of 50 μm in thickness, the biofilm internal pH would be 3.1. As indicated in the article (Torres et al., 2008), this is only a rough evaluation of the possible minimal pH inside the biofilm. Such a low pH would severely hinder bacterial growth, but the internal pH of the biofilm is surely damped by the buffer capacity of the medium. This theoretical very minimal value has only a qualitative meaning by indicating the possible drastic acidification of the biofilm during the anodic phase.

The low pH that was reached at the end of the anodic phase favored the thermodynamics of oxygen reduction (Reaction 2), which explained the high current density obtained at the beginning of the biocathode phase. Then, the production of hydroxide ions due to oxygen reduction slowly balanced out the protons accumulated inside the biofilm and, finally, resulted in an excess of hydroxide ions that have to diffuse out of the biofilm when the biocathode reached its final steady state. The slow decrease of the reduction current observed during day 35 would correspond to the slow pH increase inside the biofilm from a status of proton excess (favorable to oxygen reduction) to a status of hydroxide ions excess (detrimental to oxygen reduction). This transient state lasted 24 h (Fig. 2 – zone 1) before the current reached a stable value of 0.071 A/m^2 (day 36).

From day 38 to day 42, aeration was switched off and the reactors were left open to the air. The measured dissolved oxygen concentration corresponded to around 100% air saturation (6.5 mg/L at 40 °C) during the first phase of forced aeration, but it fell to 42 ± 1% when the forced aeration was stopped and the reactors were simply open to the air. The stable current density decreased to 27 mA/m^2 (Fig. 2), i.e., in a proportion (38%) similar to that of the oxygen concentration. It was thus confirmed that the current density was directly linked to the dissolved oxygen concentration.

Finally, when the forced aeration was turned on again on day 42 (Fig. 2 – zone 2), the current density stabilized directly to the previous steady state value (71 mA/m^2). No transient high current was observed as had been the case on day 35 when the forced aeration was established just after the bioanode phase. When there was no preceding anode phase, and consequently no proton accumulation before the forced aeration was established, no high transient current was observed. This last event confirmed the beneficial effect of anode–cathode sequencing and it supports the theory that proton accumulation is the source of cathodic current enhancement.

The electrocatalytic properties of the biocathodes were characterized by cyclic voltammetries (Fig. 3). The voltammograms performed initially (A) with the clean electrode at the initial pH of the medium (pH 7.8) showed a reproducible reduction wave starting at around −0.30 V vs. SCE. Under forced aeration, the general

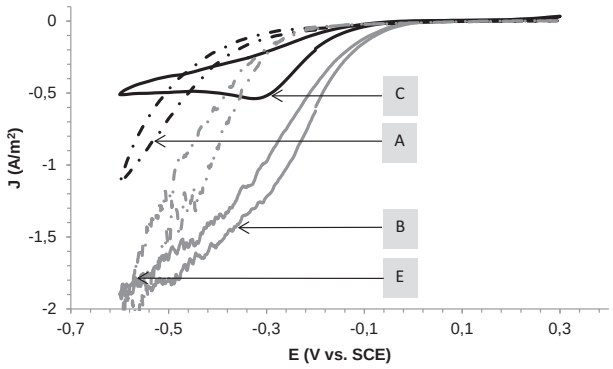

Fig. 3. Voltammograms (scan rate 1 mV/s) of the electrode in reactor 1 formed on carbon cloth at −0.20 V vs. SCE during cathodic phase. (A) Initial CV on the clean electrode (abiotic) without forced aeration (pH 7.8), (E) initial CV on the clean electrode (abiotic) with forced aeration (pH 7.8) (B) CV (day 23, pH of the medium 9.3) with forced aeration, (C) CV (day 43, pH of the medium 9.9) without forced aeration.

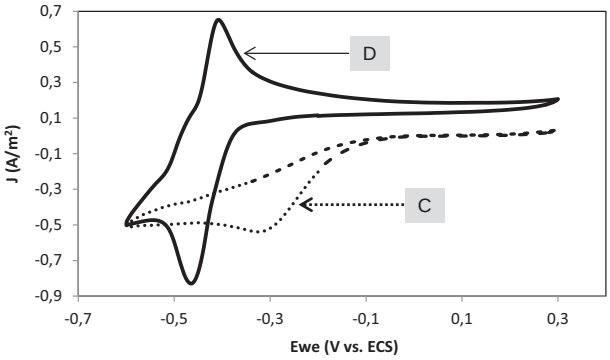

Fig. 5. Voltammograms (scan rate 1 mV/s) of the bioelectrode in reactor 1 formed on carbon cloth at −0.20 V vs. SCE. (C) CV after 43 days at the end of a cathodic phase, and (D) Non-turnover CV on day 34 at the end of an anodic phase when acetate was depleted.

shape of the reduction wave was not modified (E), the starting potential was approximately identical, but currents densities were increased. These current–potential curves corresponded to the abiotic electrochemical reduction of dissolved oxygen on the clean carbon cloth electrode.

After 43 days of biofilm formation, the biocathode produced an oxygen reduction wave starting around −0.15 V vs. SCE, and with a diffusion-limited current plateau of 530 mA/m^2 from −0.30 V vs. SCE. With the forced aeration, the limiting-current disappeared and current densities reached values as high as 1260 mA/m^2 at −0.30 V vs. SCE. The current was consequently limited by the concentration of dissolved oxygen and/or mass transfer of oxygen to the electrode surface (Fig. 3).

The voltammograms of the biocathode presented in Fig. 3 were recorded when the medium had pH values higher than 9, while the initial abiotic controls were performed with the initial pH value of 7.8. From a thermodynamic point of view, the pH value was detrimental to the biocathodes in comparison to the abiotic controls. Nevertheless, despite the possible detrimental effect of pH, the biocathodes produced more effective oxygen-reduction kinetics than the clean electrodes: reduction waves started at higher potential and current densities were significantly higher. Moreover, voltammograms were recorded at days 23 and 43, which means several days after being switched to cathodic phase. The biocathodes were consequently in a stationary state and did not benefit from the enhancing effect of biofilm acidification during the anodic phase. These voltammograms represented the stationary characteristics of the biocathodes apart for the biofilm acidification impact. It can be concluded that acidification during the anodic phase clearly enhanced the biocathode properties, but was far from being the sole cause of the entire catalytic effect. The biocathodes catalyze oxygen reduction and the biofilm acidification due to the anodic phase had a boost effect.

To evaluate the sole effect of pH on cathodic current, abiotic cyclic voltammetries were run with clean carbon cloth electrodes in the same medium at different pH: 5.3; 7.8 and 9.9 without (Fig. 4a) and with forced aeration (Fig. 4b). The pH of 5.3 was chosen to be reasonably representative of the internal biofilm acidification, without inducing to important damages to the microbial community. Previous experiments showed that the bioanodes lost drastically their performance when the pH of the medium was decreased below 5. At the potential of −0.20 V vs. SCE, cathodic current increased from 13 mA/m^2 to 66 mA/m^2 when pH decreases from 9.9 to 5.3. Forced aeration into the reactor did not significantly modify the current–potential characteristics. In these conditions and in this potential range, oxygen reduction was controlled by the electron transfer kinetics and not by oxygen transfer.

These abiotic controls confirmed that the effect of pH on abiotic reduction of oxygen was limited. At −0.20 V vs. SCE the abiotic reduction of oxygen on carbon cloth immerged in compost leachate was too slow and fully controlled by the electron transfer kinetics to be highly sensitive to the thermodynamic conditions. The impact of acidification during the anodic phase had a so important effect (enhancing current density from 70 to 400 mA/m^2) because of the biotic character of the cathode.

The capability of the same biofilm to catalyze both acetate oxidation and oxygen reduction is illustrated in Fig. 5 by overlaying a CV at the end of the anodic phase (D) on a CV at the end of a cathodic phase (C). In the range of potential values from −0.1 to −0.5 V vs. SCE, depending on whether the electrode was provided with

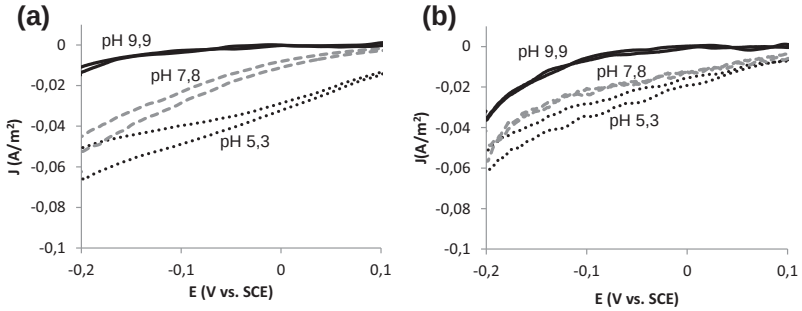

Fig. 4. Zoom-in on voltammograms (scan rate 1 mV/s) of abiotic control on carbon cloth at 3 different pH: 5.3; 7.8 and 9.9 without forced aeration (a) and with forced aeration (b).

Table 1
Diversity indexes for the initial garden compost leachate, the bulks and biofilms.

Sample	OTUs number	Simpson
T0-inoc	263	0.94
Bulk 1	370	0.88
Bulk 2	274	0.95
Biofilm 1	242	0.88
Biofilm 2	195	0.83

acetate or oxygen, the bioelectrode was able to achieve either the oxidation of acetate or the reduction of oxygen. At the end of the anodic phase, the CV was characteristic of a very efficient bioanode with a highly dominant redox couple centred at −0.44 V vs. ECS, which is in the same range of potential as the redox couples determined with different bioanodes made from *Geobacter sulfurreducens* pure culture, for instance (Fricke et al., 2008; Zhu et al., 2012). In return, at the end of the reduction phase, the electrode took on the conventional characteristics of an oxygen-reducing cathode.

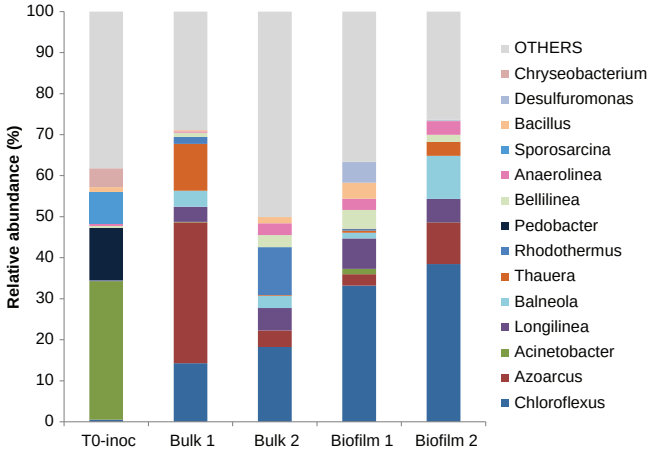

Fig. 6. Relative abundance of dominant microbial genera for the initial garden compost leachate (T0-inoc), for the bulks and biofilms 1 and 2 (duplicates). Groups that were observed at less than 2% average abundance are grouped as others.

3.3. Microbial community analyses

After trimming, sorting, and quality control, a total of 45569 sequences with an average read length of 487 nucleotides were used in downstream analysis. 25% of these sequences represented hits from the blast results that fell below 77% identity, which is not sufficient to have confidence in the determination of an organism. 34066 sequences remained and were clustered into 623 operational taxonomic units (OTUs) at 3% distance threshold. They were used in the calculations of the diversity index for each sample.

The number of organizational taxonomic units (OTUs) (Table 1) showed that the microbial communities composing the biofilms were less rich than the communities of the initial medium and the bulks at the end of the experiments (43 days chronoamperometry). The Simpson Indexes confirmed the lower diversity of the biofilm microbial communities, where the average value was 0.85 compared with 0.91 for the bulks and 0.94 for the initial garden compost leachate. These results indicated a selection of some microbial groups on the electrodes by the applied potential and/or by the cultivation conditions.

Table 2 gives the microbial communities (distribution in percentage of total sequences) at the phylum and class levels for the bulks and the biofilms of the two reactors (duplicates) at the end of experiments. In the initial garden compost leachate (T0-inoc), the dominant phyla were Proteobacteria (55%, including a majority of Gammaproteobacteria), Bacteroidetes (24%) and Firmicutes (13%). The microbial communities of the electrode biofilms were both drastically dominated by Chloroflexi (49 ± 1%) whereas enrichment in Chloroflexi was visible to a lesser extent in the bulks and may have been due to detachment of the cells from the biofilm into the solution.

At the genus level (Fig. 6) the inoculum was dominated by *Acinetobacter* sp. (34%) from the class of Gammaproteobacteria and *Pedobacter* sp. (13%) belonging to the class of Bacteroidetes. At the end of the experiments, microbial communities had radically changed and these genera represented less than 1% in biofilms and bulks. The biofilm communities were dominated by *Chloroflexus* sp. (33% and 38% for Biofilm1 and Biofim2 respectively). *Longilinea* sp., *Bellilinea* sp. and *Anaerolinea* sp., all belonging to the phylum Chloroflexi, together made up 14.7% of the population for Biofilm 1 and 10.8% for Biofilm 2.

Azoarcus sp. (34%) from the class of Betaproteobacteria dominated the microbial community of the bulk 1, while bulk 2 presented a more diverse microbial community, as indicated by the relatively high Simpson index (Table 1).

Bioanodes that were formed under identical conditions (garden compost leachate as inoculum, acetate as substrate, polarization at −0.2 V vs. SCE), but in anaerobic conditions (no aeration phase) led to microbial communities dominated by Proteobacteria with 73% ± 2% at the electrode and 51% ± 1% in the bulks. Among Proteobacteria, an enrichment of the biofilms in Deltaproteobacteria was noticeable. Microbial 16S rRNA pyrosequencing gave a relative abundance of 27% ± 4% of Deltaproteobacteria at the anode whereas it was only 1.5% ± 0.5% in the bulks. Chloroflexi composed less than 0.3% of these populations (data to be published). This kind of microbial composition was fully consistent with the analysis commonly reported for bioanodes, with dominance of Proteobacteria (Logan and Regan, 2006).

It can be concluded that the reversible anode–cathode phases led to the selection of a specific microbial community dominated by Chloroflexi. This phylum has not been frequently found in bioelectrochemical systems. Chloroflexi has previously been identified on the anode of an MFC powered by rhizodeposits of living rice plants, but it represented only 6% of all clones (Schamphelaire et al., 2010). Chloroflexi have also been found enriched on the anode of a cellulose-fed MFC (Ishii et al., 2008). The high

Table 2
Microbial community (distribution in percentage of total sequences) at the class level. T0-inoc is the initial medium. 1 and 2 indicate two reactors run in parallel during 43 days of polarization at −0.20 V vs. SCE.

Phylum	Chloroflexi (%)		Proteobacteria (%)				Firmicutes (%)	Bacteroidetes (%)	Others
Class	Chloroflexi (class)	Anaerolineae	α	β	γ	δ			
T0-inoc	1	1	11	5	38	1	13	24	5
Bulk 1	14	5	11	49	1	4	4	4	7
Bulk 2	18	12	11	5	4	4	13	10	23
Biofilm 1	33	15	8	8	3	3	10	12	7
Biofilm 2	39	11	8	16	1	11	1	5	8

percentages found here in both duplicates indicate that Chloroflexi may be a characteristic of reversible bioanodes.

Chloroflexi are known as green non-sulfur bacteria. They are generally photoheterotrophs and can use various sugars and organic acids as electron donors. This metabolism would give them the possibility to develop during anodic phases when acetate is available, using the electrode as electron acceptor. Moreover, Chloroflexi are facultative aerobic, which means that they can develop during the biocathode phase and they have the enzymatic equipment to reduce oxygen. Such a flexible metabolism is a selective advantage for Chloroflexi over other microbial strains, and certainly explains their dominance at the electrodes.

Chloroflexus sp. is a filamentous organism abundant in wastewater treatment plant (Björnsson et al., 2002). It can be speculated that, given its filamentous aspect, *Chloroflexus species* might play a role in electron transport. A similar phenomenon has been described by Pfeffer et al. (2012) for members of the Desulfobulbaceae family. This study showed that long-distance electron transport from sulfide to oxygen was possible in sediment, mediated by the micro-cables that form the long filamentous bacteria. Nevertheless, to the best of our knowledge there is no proof of the possible electroactivity of Chloroflexi in the literature so far. One of the main conclusions of the present work is that the possible electroactivity of Chloroflexi should now be considered as a major scientific question, because they may represent an essential pillar in the design of very efficient reversible bioelectrodes.

4. Conclusion

Reversible bioelectrodes are an appealing approach boosting the performance of MFCs by using the accumulation of protons, which limits the bioanode operation, as an advantage to favor the biocathode operation. The success of this strategy was demonstrated here with bioanodes formed from garden compost. The microbial community that composed the reversible bioelectrodes was dominated by Chloroflexi, a class of bacteria known as filamentous green non-sulfur bacteria, facultative aerobic, which now deserves further fundamental investigation as a possible candidate for the design of reversible bioelectrodes with pure culture.

Acknowledgements

This work was part of the "BIORARE" Project (ANR-10-BTBR-02), partly funded by the French Agence Nationale de la Recherche (ANR) and the Comité des Investissements d'Avenir. We thank Luc Etcheverry and Mickaël Rimboud (Toulouse, France) for their kind contributions.

References

Bergel, A., Féron, D., Mollica, A., 2005. Catalysis of oxygen reduction in PEM fuel cell by seawater biofilm. Electrochem. Commun. 7, 900–904.

Björnsson, L., Hugenholtz, P., Tyson, G.W., Blackall, L.L., 2002. Filamentous Chloroflexi (green non-sulfur bacteria) are abundant in wastewater treatment processes with biological nutrient removal. Microbiology 148, 2309–2318.

Borole, A.P., Reguera, G., Ringeisen, B., Wang, Z.-W., Feng, Y., Kim, B.H., 2011. Electroactive biofilms: current status and future research needs. Energy Environ. Sci. 4, 4813–4834.

Carbajosa, S., Malki, M., Caillard, R., Lopez, M.F., Palomares, F.J., Martín-Gago, J.A., Rodríguez, N., Amils, R., Fernández, V.M., De Lacey, A.L., 2010. Electrochemical growth of *Acidithiobacillus ferrooxidans* on a graphite electrode for obtaining a biocathode for direct electrocatalytic reduction of oxygen. Biosens. Bioelectron. 26, 877–880.

Cercado, B., Byrne, N., Bertrand, M., Pocaznoi, D., Rimboud, M., Achouak, W., Bergel, A., 2013. Garden compost inoculum leads to microbial bioanodes with potential-independent characteristics. Bioresour. Technol. 134, 276–284.

Cercado-Quezada, B., Delia, M.-L., Bergel, A., 2010. Treatment of dairy wastes with a microbial anode formed from garden compost. J. Appl. Electrochem. 40, 225–232.

Cheng, K.Y., Ho, G., Cord-Ruwisch, R., 2010. Anodophilic biofilm catalyzes cathodic oxygen reduction. Environ. Sci. Technol. 44, 518–525.

Dowd, S.E., Callaway, T.R., Wolcott, R.D., Sun, Y., McKeehan, T., Hagevoort, R.G., Edrington, T.S., 2008. Evaluation of the bacterial diversity in the feces of cattle using 16S rDNA bacterial tag-encoded FLX amplicon pyrosequencing (bTEFAP). BMC Microbiol. 8, 125.

Dumas, C., Mollica, A., Féron, D., Basseguy, R., Etcheverry, L., Bergel, A., 2008. Checking graphite and stainless anodes with an experimental model of marine microbial fuel cell. Bioresour. Technol. 99, 8887–8894.

Edgar, R.C., 2010. Search and clustering orders of magnitude faster than BLAST. Bioinformatics 26, 2460–2461.

Edgar, R.C., Haas, B.J., Clemente, J.C., Quince, C., Knight, R., 2011. UCHIME improves sensitivity and speed of chimera detection. Bioinformatics 27, 2194–2200.

Erable, B., Féron, D., Bergel, A., 2012. Microbial catalysis of the oxygen reduction reaction for microbial fuel cells: a review. ChemSusChem 5, 975–987.

Fan, Y., Sharbrough, E., Liu, H., 2008. Quantification of the internal resistance distribution of microbial fuel cells. Environ. Sci. Technol. 42, 8101–8107.

Freguia, S., Rabaey, K., Yuan, Z., Keller, J., 2008. Sequential anode–cathode configuration improves cathodic oxygen reduction and effluent quality of microbial fuel cells. Water Res. 42, 1387–1396.

Fricke, K., Harnisch, F., Schröder, U., 2008. On the use of cyclic voltammetry for the study of anodic electron transfer in microbial fuel cells. Energy Environ. Sci. 1, 144.

Harnisch, F., Schröder, U., 2009. Selectivity versus mobility: separation of anode and cathode in microbial bioelectrochemical systems. ChemSusChem 2, 921–926.

Ishii, S., Shimoyama, T., Hotta, Y., Watanabe, K., 2008. Characterization of a filamentous biofilm community established in a cellulose-fed microbial fuel cell. BMC Microbiol. 8, 6.

Ketep, S.F., Bergel, A., Calmet, A., Erable, B., 2014. Stainless steel foam increases the current produced by microbial bioanodes in bioelectrochemical systems. Energy Environ. Sci. 7, 1633.

Ketep, S.F., Fourest, E., Bergel, A., 2013. Experimental and theoretical characterization of microbial bioanodes formed in pulp and paper mill effluent in electrochemically controlled conditions. Bioresour. Technol. 149, 117–125.

Li, W., Sun, J., Hu, Y., Zhang, Y., Deng, F., Chen, J., 2014. Simultaneous pH self-neutralization and bioelectricity generation in a dual bioelectrode microbial fuel cell under periodic reversion of polarity. J. Power Sources 268, 287–293.

Logan, B.E., Regan, J.M., 2006. Electricity-producing bacterial communities in microbial fuel cells. Trends Microbiol. 14, 512–518.

Parot, S., Nercessian, O., Delia, M.-L., Achouak, W., Bergel, A., 2009. Electrochemical checking of aerobic isolates from electrochemically active biofilms formed in compost. J. Appl. Microbiol. 106, 1350–1359.

Pfeffer, C., Larsen, S., Song, J., Dong, M., Besenbacher, F., Meyer, R.L., Kjeldsen, K.U., Schreiber, L., Gorby, Y.A., El-Naggar, M.Y., Leung, K.M., Schramm, A., Risgaard-Petersen, N., Nielsen, L.P., 2012. Filamentous bacteria transport electrons over centimetre distances. Nature 491, 218–221.

Pocaznoi, D., Calmet, A., Etcheverry, L., Erable, B., Bergel, A., 2012a. Stainless steel is a promising electrode material for anodes of microbial fuel cells. Energy Environ. Sci. 5, 9645–9652.

Pocaznoi, D., Erable, B., Etcheverry, L., Delia, M.-L., Bergel, A., 2012b. Towards an engineering-oriented strategy for building microbial anodes for microbial fuel cells. Phys. Chem. Chem. Phys. 14, 13332–13343.

Rimboud, M., Pocaznoi, D., Erable, B., Bergel, A., 2014. Electroanalysis of microbial anodes for bioelectrochemical systems: basics, progress and perspectives. Phys. Chem. Chem. Phys. 16, 16349–16366.

Rozendal, R.A., Hamelers, H.V.M., Rabaey, K., Keller, J., Buisman, C.J.N., 2008. Towards practical implementation of bioelectrochemical wastewater treatment. Trends Biotechnol. 26, 450–459.

Santoro, C., Babanova, S., Atanassov, P., Li, B., Ieropoulos, I., Cristiani, P., 2013. High power generation by a membraneless single chamber microbial fuel cell (SCMFC) using enzymatic bilirubin oxidase (BOx) air-breathing cathode. J. Electrochem. Soc. 160, H720–H726.

Schamphelaire, L.D., Cabezas, A., Marzorati, M., Friedrich, M.W., Boon, N., Verstraete, W., 2010. Microbial community analysis of anodes from sediment microbial fuel cells powered by rhizodeposits of living rice plants. Appl. Environ. Microbiol. 76, 2002–2008.

Strik, D.P.B.T.B., Hamelers, H.V.M., Buisman, C.J.N., 2010. Solar energy powered microbial fuel cell with a reversible bioelectrode. Environ. Sci. Technol. 44, 532–537.

Strik, D.P.B.T.B., Hamelers (Bert), H.V.M., Snel, J.F.H., Buisman, C.J.N., 2008. Green electricity production with living plants and bacteria in a fuel cell. Int. J. Energy Res. 32, 870–876.

Torres, C.I., Kato Marcus, A., Rittmann, B.E., 2008. Proton transport inside the biofilm limits electrical current generation by anode-respiring bacteria. Biotechnol. Bioeng. 100, 872–881.

Zhu, X., Yates, M.D., Logan, B.E., 2012. Set potential regulation reveals additional oxidation peaks of *Geobacter sulfurreducens* anodic biofilms. Electrochem. Commun. 22, 116–119.